Host-pathogen transcriptomics of macrophages, Mucorales and their endosymbionts: a polymicrobial pas de trois

Authors

Poppy Sephton-Clark[1], José F Muñoz[2], Herbert Itabangi[1], Kerstin Voelz[1], Christina A Cuomo[2], Elizabeth R Ballou[1]*

[1]*Institute of Microbiology and Infection, School of Biosciences, University of Birmingham, Edgbaston, Birmingham, B15 2TT, UK*

[2]*Infectious Disease and Microbiome Program, Broad Institute of MIT and Harvard, Cambridge, Massachusetts, USA*

* To whom correspondence should be addressed
ERB: e.r.ballou@bham.ac.uk

Abstract

Mucorales spores, the causative agents of mucormycosis, interact with the innate immune system to cause acute, chronic, or resolving infection. Understanding the factors that influence disease initiation and progression is key to understanding mucormycosis and developing new treatments. Complicating this, mucormycosis can be caused by a number of species that span the Mucorales genus and may be host to bacterial endosymbionts. This study sets out to examine the differences between two species in the Mucorales order by characterising their differential interactions with the innate immune system, and their interactions with environmental bacterial endosymbionts. Through a holistic approach, this study examines the transcriptional responses of *Rhizopus delemar* and *Rhizopus microsporus,* two of the most commonly diagnosed species, to innate immune cells. This study also examines the immune cell response and assesses the variation in these responses, given the presence or absence of bacterial endosymbionts within the fungi. We see that the fungal response is driven by interaction with innate immune cells. The effect of the bacterial endosymbiont on the fungus is species specific, with a minimal in the absence of stress, but strongly influencing fungal transcripts during interaction with innate immune cells. In contrast, we observe that the macrophage response varies depending on the infecting fungal species, but also depending on endosymbiont status. The most successful macrophages elicit a pro-inflammatory response, and we see that through germination inhibition macrophage survival is enhanced. This work reveals species-specific host responses to related Mucorales spores and shows that bacterial endosymbionts impact the innate immune cell response.

Introduction

Mucormycosis is a devastating, environmentally acquired fungal infection caused by a variety of Mucorales species. Understanding the interaction between Mucorales spores and innate immune cells is key to understanding mucormycosis. Studies frequently focus upon the interaction of a single species of the Mucorales order with innate immune cells (Warris

et al. 2005; Chamilos et al. 2008; Schmidt et al. 2013; Kraibooj et al. 2014; Inglesfield et al. 2018). However, between Mucorales species, and across infecting isolates, numerous phenotypic and genomic differences can be observed (Hoffmann et al. 2013; Mendoza et al. 2014; Schwartze et al. 2014). Whether each species within this family employs the same mechanism to cause infection remains unclear, however the range of virulence profiles displayed across the family indicates there may be diversified mechanisms at work (Petraitis et al. 2013). For example, it has been shown that pathogenicity of these species is linked to the variable copy number of the gene encoding CotH, a family of cell surface proteins important for the spores' interactions with and adherence to endothelial cells. Iron-scavenging and melanisation pathways have also been shown to play a role in pathogenicity (Chibucos et al. 2016, Andrianaki et al. 2018). In addition to fungal genome plasticity and transcriptional responses to host stimuli, fungal-host interactions can be further modulated by bacterial endosymbionts (Itabangi et al., 2019; Partida-Martinez & Hertweck 2005). The majority of Mucorales species have been shown to harbour bacterial endosymbionts whose species can vary between Mucorales isolates (Ibrahim et al. 2008; Kobayashi & Crouch 2009; Mondo et al. 2017; Itabangi et al. 2019). We have recently shown that a bacterial endosymbiont influences the outcome of *Rhizopus microsporus* infections in both zebrafish and murine models through modulation of both fungal and phagocyte phenotypes (Itabangi et al. 2019). However, the impact of endosymbiont on fungal and host transcriptional response remains unclear.

While disease can be caused by several species in the Mucorales order, *Rhizopus delemar* and *Rhizopus microsporus* are responsible for the majority of infections (Liu et al. 2018). Risk factors for developing the disease include, but are not limited to: innate immune cell deficiencies, uncontrolled diabetes, immune suppression, skin barrier breaches and iron overload (Baldin & Ibrahim 2017). With limited antifungal treatments effective against these invasive infections, there is often a need for surgical debridement or amputation (Spellberg et al. 2016). In disseminated cases, mucormycosis may present with a mortality rate of over 90% (Mendoza et al. 2014). Reports of chronic mucormycosis have also emerged, affecting both immunocompromised and immunocompetent patients (Alan et al. 2019). The innate immune response to Mucorales spores is key to infection control: macrophages are required to induce a differential immune response on contact with *Rhizopus* spp. and may inhibit germination or kill hyphal forms upon contact in healthy individuals (Ghuman & Voelz 2017; Andrianaki et al. 2018). Single and multi-species studies have shown that phagosome maturation is arrested by melanin within the cell walls of *Aspergillus* spp. and *Rhizopus* spp., however iron limitation allows macrophages to more effectively kill *Rhizopus* spp.(Liu et al. 2015; Ibrahim et al. 2010; Andrianaki et al. 2018). Several works comparing *Aspergillus* spp. to *Rhizopus* spp. have revealed similar immunostimulatory capacities, but differences in their responses to host stress (Warris et al. 2005; Chamilos et al. 2008; Schmidt et al. 2013; Kraibooj et al. 2014). Exploring and understanding fungal responses to the host is essential to improving our understanding of mucormycosis, yet it remains unclear how Mucorales species respond to, and interact with, the innate immune system, and to what extent this varies by species.

Our work explores the interplay between the innate immune system, *R. delemar,* and *R. microsporus* using isolates of both species found to harbour bacterial endosymbionts (Itabangi et al. 2019). We investigate the differences between these two fungal species, how

they respond transcriptionally to innate immune cells, and how their respective bacterial endosymbionts affect this interaction. We also investigate the transcriptional response of innate immune cells to these infectious spores and determine how this interaction is influenced by the presence of an endosymbiont. We reveal a large difference between the fungal transcriptional profiles of *R. delemar* and *R. microsporus* during *in vitro* monoculture. There is a small conserved response to exposure to innate immune cells, including key changes in cell wall genes, consistent with germination. Conversely, we see that the host innate immune response differs significantly between fungal species and is also influenced by the presence or lack of an endosymbiont. The innate immune response to *R. delemar* and *R. microsporus* mirrors the relative aggressiveness of infection between these two species. We also observe that through the activation of innate immune cells, or upon inhibition of chitin synthase, we can improve the ability of innate immune cells to control the fungal spores. Our work represents a broad analysis of the transcriptional interplay between innate immune responders and infectious Mucorales spores, revealing species-species differences which question the current model of 'one species represents all', when it comes to mucormycosis.

Results

Experimental Design

We set out to investigate paired transcriptional responses of host and fungal cells, whilst also exploring the influence of the endosymbiont on this interaction (Figure 1a). Fungal spores from *Rhizopus delemar* and *Rhizopus microsporus* were either cured via ciprofloxacin treatment to remove the bacterial endosymbiont (cured) or maintained in media permissive to bacterial endosymbiosis (wt). Cured spores were passaged twice in the absence of ciprofloxacin to limit the impact of the drug on transcriptional responses. The cured and wt spores of both *R. delemar* and *R. microsporus* were allowed to swell in sabouraud broth until 95% of the population had reached mid isotropic phase. Due to the differences in germination rates between the species (Figure 1b), this occurred at 2 hours for *R. delemar* and 4 hours for *R. microsporus.* Swollen spores were then used to infect the J774.1 murine macrophage-like cell line. Fungal spores were co-cultured with macrophages for one hour, after which unengulfed spores were removed, and phagocytosed spores were incubated within the macrophages for a further two hours. The cells from the resulting infection were processed to explore their transcriptional response to this infection scenario (Figure 1a). Macrophages that had phagocytosed fungal spores were isolated and sequenced via the 10X Genomics Chromium Single Cell Sequencing platform. Macrophages left unexposed to the fungi were used as a negative control. RNA was also isolated from fungal spores (cured and wt) which had been engulfed by macrophages, and this was sequenced with a bulk RNA-Seq approach. Unexposed fungi (cured and wt) were incubated in macrophage media for a matched time and used as a negative control. The data shows the fungal response to phagocytosis by macrophages, as well as the fungal response to the presence of its endosymbiont. The macrophage response to the two species is also revealed, a response which appears to differ when the endosymbiont is present for both fungal species.

Comparative genomics predicts alternative transcriptional responses

In order to better understand differential disease progression, we chose to compare *R. delemar* and *R. microsporus*, as they cause a large proportion of mucormycosis infections but appear morphologically dissimilar. *R. delemar* germinates more quickly than *R. microsporus*, with 50% of spores germinating by 3 hours, and a spore body size which reaches 12.8 μm over the course of germination (Figure 1b, c). *R. microsporus* germinates at a significantly slower rate, taking 6 hours for 50% of spores to germinate, with a final spore body size of 13.9 μm (Figure 1b, c). To better understand their relationship to one another, we compared the gene content to explore the similarity and differences between the two species. Previous work has established that the *R. delemar* genome (45.3 Mb, 17,513 genes) is larger, and contains an increased number of genes, compared to *R. microsporus* genome (26 Mb, 10,959 genes) (Ma et al. 2009; Mondo et al. 2017). Our results show that, compared to *R. microsporus*, the genome of *R. delemar* is enriched for genes with protein domains (PFAM) associated with ion binding, carbohydrate derivative binding, nucleic acid binding, cytoskeletal protein binding, poly(A) binding, NAD+ ADP-ribosyltransferase activity, protein kinase C activity, translation initiation factor binding and inorganic phosphate transmembrane transporter activity (Supplemental Figure S1, Figure 1d). *R. microsporus* is enriched for genes with protein domains corresponding to nucleoside phosphate binding, early endosome activity and DNA repair complex activity (Supplemental Figure S1, Figure 1d). The clear differences illustrated by genome size and gene content indicate the likelihood of alternative transcriptional responses.

Alternative transcriptional profiles are presented by *R. delemar* and *R. microsporus* in response to innate immune cells

First we examined overall trends in fungal responses to phagocytosis, obtained through our bulk RNA-Seq approach. We analysed the signal obtained from *R. delemar* and *R. microsporus* samples with principle component analysis (PCA) (Figure 2). We observed large differences between the transcriptomes of both fungal species, when exposed or unexposed to macrophages, while the presence or absence of their respective endosymbionts had a weak but differential effect on PCA. The presence or absence of the endosymbiont appears to have very little bearing on the transcriptional patterns displayed by *R. delemar*, as samples fell into two distinct clusters, most strongly influenced by macrophage status (Figure 2a). *R. microsporus* exhibits a similar trend upon exposure to macrophages, however the presence of the endosymbiont also influenced clustering (Figure 2b). We investigate the phenotypic consequences of this interaction in the companion paper by Itabangi et al., showing that the presence of the endosymbiont *Ralstonia pickettii* impacts fungal cell wall organization, resistance to host-relevant stress, spore germination efficiency, and pathogenesis (Itabangi et al., 2019). Therefore, we focus here on the transcriptional analysis of the host-pathogen-endosymbiont interaction across the two species.

There are 2,493 genes that are significantly differentially expressed (Log fold change > 2; false discovery rate < 0.05) in *R. delemar* across all conditions (Figure 3a), while *R. microsporus* only exhibits 40 genes significantly differentially expressed across all conditions (Log fold change > 2; false discovery rate < 0.05) (Figure 3b). The theme of a muted

184 transcriptional response from *R. microsporus* is also seen within pairwise comparisons of
185 conditions. Pairwise comparisons of differential expression across each experimental
186 condition show similar trends in responses between *R. delemar* and *R. microsporus*,
187 however *R. microsporus* responds with a reduced gene set (Figure 4). Pairwise comparisons
188 showed the biggest shift in transcriptional response when comparing phagocytosed fungal
189 spores to those unexposed to macrophages, regardless of endosymbiont status. When
190 phagocytosed (Supplemental Figure S2), *R. microsporus* upregulates genes enriched in GO
191 categories corresponding to thiamine metabolism, sulfur metabolism, glycerol metabolism,
192 alcohol dehydrogenase activity and transmembrane transporter activity (hypergeometric
193 test, corrected *P* value < 0.05). This is consistent with the fungal response seen to
194 macrophage stress (Parente-Rocha et al. 2015), and the micronutrient scavenging response
195 to nutritional immunity (Ballou and Wilson 2016; Shen et al., 2018; Andrianaki et al., 2018).
196 Phagocytosed *R. microsporus* downregulated genes enriched in GO categories
197 corresponding to rRNA processing, ribosome biogenesis and ribosome localization
198 (hypergeometric test, corrected *P* value < 0.05) (Supplemental Figure S2), consistent with
199 growth arrest within the phagolysosome (Inglesfield et al. 2018; Andrianaki et al. 2018).
200
201 Comparisons of *R. delemar* conditions reveal that, upon phagocytosis, spores upregulate
202 genes enriched in KEGG classifications corresponding to MAPK signalling, phenylalanine
203 metabolism, tyrosine metabolism, glutathione metabolism and fatty acid synthesis
204 (hypergeometric test, corrected *P* value < 0.05). Upregulation of these processes is
205 consistent with melanin biosynthesis (Eisenman et al. 2011; Andrianaki et al. 2018) and
206 intra-phagosomal survival (Yadav et al., 2011; Lorenz and Fink, 2005). Unexposed *R. delemar*
207 spores upregulate genes enriched in KEGG classifications corresponding to ketone body
208 synthesis, protein processing via the endoplasmic reticulum, amino sugar and nucleotide
209 sugar metabolism (hypergeometric test, corrected *P* value < 0.05). This is consistent with
210 metabolic activation and cell wall biogenesis (Figure 5).
211
212 *R. delemar* and *R. microsporus* harbour distinct bacterial endosymbionts (Itabangi et al.,
213 2019). When comparing transcriptional profiles of wt and cured spores incubated in serum-
214 free DMEM (sfDMEM) for 3 hours (time matched to phagocytosis assay), we observed very
215 few transcriptional changes in either species in response to curing (Supplemental Table 1).
216 In *R. delemar,* a single gene, predicted to be a putative protein phosphatase, was repressed.
217 In *R. microsporus,* three genes were induced: an autophagy-related protein, a C2H2 zinc
218 finger transcription factor, and ribosomal protein L2.
219
220 Despite these small changes, loss of the endosymbiont significantly impacted the
221 transcriptional responses of both fungal species to macrophages (Figure 4). Specifically, we
222 observed an overall increase in the number of fungal genes differentially regulated upon
223 phagocytosis for both species. Exposure of wt *R. microsporus* to macrophages induced the
224 expression of one gene with no known function and repressed 6 genes. The repressed genes
225 include an autophagy-related protein and a zinc finger transcription factor, as well as 4 un-
226 annotated genes (Figure 4, Supplemental Table S1). In contrast, when cured *R. microsporus*
227 spores were exposed to macrophages, 277 genes were significantly induced and 82
228 repressed, compared to unexposed cured spores (Figure 4). Induced genes were enriched
229 (hypergeometric test, corrected *P* value < 0.05) for the following GO categories: organelle
230 organisation, pre-ribosome and ribosome activity, ATPase activity, hydrolase activity,

231 pyrophosphatase activity, helicase activity, nucleic acid binding, RNA metabolism, nitrogen
232 metabolism, chromatin silencing. Repressed genes were enriched (hypergeometric test,
233 corrected *P* value < 0.05) for the following GO categories: oxidoreductase activity, hydrogen
234 sulphide metabolism, glycolysis, sulphur metabolism, hexose catabolism, siderophore activity,
235 iron assimilation, nitrogen metabolism, carboxylic acid metabolism. This suggests an overall
236 failure to properly respond to host stresses such as iron starvation in the absence of the
237 bacterial endosymbiont.
238
239 A similar impact of the endosymbiont was observed for *R. delemar.* While the overall fungal
240 response to phagocytosis is characterized by a robust transcriptional response, induced
241 genes in wt samples (1137 genes, Figure 4) were enriched for KEGG classifications
242 corresponding to: alanine metabolism, PPAR signalling, aromatic compound biosynthesis
243 and degradation, lysine metabolism, lipid metabolism, MAPK signalling, sugar metabolism,
244 tyrosine metabolism, secondary metabolite biosynthesis (Figure 5). Repressed genes in wt
245 samples (472 genes, Figure 4) were enriched for KEGG classifications corresponding to:
246 carbohydrate metabolism, secondary metabolite biosynthesis, ketone body processing,
247 protein processes, MAPK signalling (Figure 5). In contrast, induced genes in cured samples
248 (1285 genes, Figure 4) were enriched for KEGG classifications corresponding to: Fatty acid
249 metabolism, DNA replication, amino acid metabolism, glycan metabolism, pyruvate
250 metabolism, secondary metabolite processing (Figure 5). Repressed genes in cured samples
251 (878 genes, Figure 4) were enriched for KEGG classifications corresponding to: sugar
252 metabolism, amino acid metabolism, lipid metabolism, MAPK signalling, NOD-like receptor
253 signalling. Again, this suggests that the endosymbiont has an overall suppressive impact on
254 fungal transcription in response to macrophage challenge.
255
256 Next, we directly compared the transcription patterns of genes shared across the two fungal
257 species. When comparing the transcriptional responses of orthologous genes shared by *R.*
258 *delemar* and *R. microsporus*, we saw only a small proportion behave similarly (213 genes).
259 When phagocytosed, wt spores from both species upregulate orthologues genes involved in
260 fatty acid catabolism, transcription, regulation via polymerase II, and organelle organization.
261 Phagocytosed cured spores from both species upregulate orthologues genes involved in
262 RNA processing, chromosome organization and condensed chromosome pathways. When
263 unexposed, we see wt spores upregulate orthologous genes involved in translocation,
264 protein binding, siderophore activity, cobalmin processing, and post-translational protein
265 targeting. Cured unexposed spores upregulate orthologous genes with roles in siderophore
266 activity and transferase activity. Overall, *R. delemar* and *R. microsporus* both respond
267 transcriptionally to the presence of macrophages, however the size and composition of this
268 response differs between species.
269
270 Finally, we examined the regulation of genes predicted to be involved in ferrous iron
271 transport, as previous work has linked iron scavenging to survival within the phagolysosome
272 (Andrianaki et al., 2018). There are 12 genes in the *R. delemar* genome with predicted
273 ferrous iron roles. While 8 showed no significant change over the tested conditions, 3
274 (R0G3_006623, R0G3_007727, R0G3_011864) appeared highly expressed in wt and cured
275 phagocytosed spores, compared to unexposed spores. The last gene, ROG3_009943, is
276 highly expressed in wt spores unexposed to macrophages. Together, this suggests there

may be condition dependent specialization in the expression of ferrous iron transport in *R. delemar*.

Innate immune cell transcription varies with fungal species and endosymbiont presence

To investigate the innate immune response when challenged with *R. delemar* and *R. microsporus*, we carried out single cell RNA-Seq of J774.A1 murine macrophages, unexposed and exposed for 3 hours to the four types of pre-swollen spores (Figure 1a). Transcription of both challenged and unchallenged macrophages displayed underlying population heterogeneity (Supplemental Figure S3). To identify the transcriptional patterns of genes responding to the spores, we focused on the expression of a subset of genes previously identified as immune response genes (Muñoz et al. 2018). Principle component analysis of the aggregated transcriptional data shows there is a clear difference in transcription between macrophages that have and have not been exposed to the fungi (Figure 6). Across all exposed conditions, relative to unexposed macrophages, there was a profile consistent with cytokine activation, response to stimulus, and activation of the NF-Kb pathway. This was accompanied by repression of CCL5, which is involved in T-cell recruitment (Figure 7). However, different macrophage profiles can be seen in response to the two fungal species, and these are further influenced by the presence of the endosymbiont. While the response to wt *R. delemar* shows the most deviation from the macrophage-only control, exposure to cured *R. delemar* also elicited a strong and distinct macrophage response (Figures 6,7). Exposure to wt *R. delemar* elicits increased expression of general markers of activation, including GTPase activity and MHC class II protein binding (LAG3 repressor of T-cell activation, H2-M2, IFN-gamma induced IIGP1, MX1, KCTD14, PNP2), growth factor binding, IL1 receptor agonist activity and endocytosis (SERPINE1, ENG, FGFBP3, GM8898, GCNT2, IL1F6). Specifically, we observe modest increases in the expression of IFN-γ responsive CXCL10 (3.1 fold) and IRG1/IRG11 (5.9 fold), pro-inflammatory SAA3 (3.5 fold), and ENPP4 (2.8 fold), but also induction of the M2 polarizing PSTPIP2/21 (6.7 fold), the IL-4 responsive signaling modulator CISH (5.4 fold), and the vascular damage responsive F3/F31 (5.9 fold) (Martinez et al. 2013). These latter genes are not as strongly induced during exposure to *R. microsporus*, which may reflect the aggressive nature of infection by *R. delemar* relative to *R. microsporus.* In contrast, infection with cured *R. delemar* showed a decrease in the induction of these M2-polarisation markers (PSTPIP2, 3.5 fold relative to uninduced). The transcriptional profile is instead shifted to include increased transcription of genes involved in G protein signaling and phosphoinositide binding (PDE7B, CCL1, SCARF1, RGS16, PLEKHA4) (Figure 7).

A similar change in macrophage polarization was observed during exposure to wt and cured *R. microsporus.* The phenotypic analysis of this is discussed more fully in Itabangi et al. 2019. For both wt and cured *R. microsporus,* expression of IFN-γ responsive CXCL10, SAA3, and ENPP4 was comparable to unexposed macrophages. Compared to *R. delemar,* exposure to wt *R. microsporus* induced a more limited expression of genes with roles in cytokine activation, ERK1 and ERK2 regulation, and regulation of NF-kB cascade (Figure 7). There was also a weaker induction of the vascular damage responsive F3/F31 genes, and a relatively stronger upregulation of the PLA2G16 phospholipase, TRIM30D, SLC1A2 and the M2 polarizing IL-6. However, other key polarizing genes, particularly PSTPIP2/21, SAA3, and

ENPP4 were only weakly induced (Supplemental Table S2). Overall, this profile suggests a weak M1-like activation consistent with poor phagocytosis and reduced overall antifungal activity that we observe in macrophages interacting with endosymbiont-harbouring spores (Itabangi et al., 2019).

Finally, cured *R. microsporus* induced a strong pro-inflammatory response, which included upregulation of CXCL3, the neutrophil chemoattractant, consistent with our observations of differences in phagocyte recruitment in zebrafish upon infection with wt vs. cured spores (Itabangi et al., 2019). Markers of NF-kB activation were also strongly induced in this population. Cured *R. microsporus* also strongly induced the expression of TNFRSF8 (CD30), a marker of lymphocyte activation occasionally associated with subcutaneous fungal infections. Overall, this is suggestive of a shift to a more pro-inflammatory profile. In our companion paper, we observed that cured *R. microsporus* is more sensitive to phagocyte-mediated killing and phagocyte recruitment compared to wt (Itabangi et al., 2019). We therefore went on to test whether a more successful response to the spores could be mounted via the induction of a pro-inflammatory response.

Chitin synthase inhibition and pro-inflammatory priming regulate infection outcome

R. delemar exhibits rapid germination followed by hyphal extension (Sephton-Clark et al., 2018). The transcriptional profile we observe here in macrophages exposed to *R. delemar* is consistent with a strong damage response, likely prompted by the germination of *R. delemar* spores. We therefore hypothesised that macrophages may be better able to control the infection if the fungi were slowed in their developmental progress. The necessity of genes involved in chitin synthesis and regulation appeared important for both *R. delemar* and *R. microsporus* in response to phagocytosis (Supplemental Figure S4). In previous work we also highlighted the importance of chitin synthase for germination (Sephton-Clark et al. 2018). When fungal spores were pre-treated with the chitin synthesis inhibitor Nikkomycin Z (24 μg/ml), spores failed to germinate, displayed less chitin/chitosan in their outer cell wall (Supplemental Figure S5) and macrophage survival was increased at 7.5 hours post infection (Figure 8). At Nikkomycin Z concentrations lower than those used to pre-treat spores for phagocytosis, we see the spores are able to swell, however development appears halted after swelling (Supplemental Figure S5). As the macrophages are better able to control these spores, this suggests that spores undergoing the initial stages of germination may offer less of a challenge for the macrophages.

Our transcriptional data show a strong M2 alternative activation signal during *R. delemar*-macrophage interaction, but a weaker M2 polarisation during *R. microsporus*-macrophage interaction that was further shifted towards NF-kB-mediated M1 upon endosymbiont cure. We therefore hypothesized that shifting the macrophage polarization towards M1 classical activation might have a protective effect upon Mucorales infection. Consistent with this, the pre-treatment of macrophages with NF-kB activating lipopolysaccharide (LPS) significantly improved the ability of macrophages to control *R. microsporus*. At 7.5 hours post infection, 59.7% of macrophages survived when pre-treated with LPS, compared to 24.6% without (Figure 8).

Discussion

In this work we show the fungal response to innate immune cells differs by species in the Rhizopodaceae family. Although *R. delemar* and *R. microsporus* share a small conserved response to exposure to macrophages, the majority of their response differs. We show that the ability to germinate prior to phagocyte control appears to be key to virulence, as blocking spore germination with the chitin synthase inhibitor Nikkomycin Z improves macrophage survival. A range of germination and virulence phenotypes can be seen throughout the Mucorales, and this highlights a need for further investigation into these differences, to better understand the infections they cause.

We have also shown that the fungal transcriptional response appears largely unperturbed by the presence, or lack, of an endosymbiont, in the absence of stress. However, the presence of an endosymbiont greatly effects the response of and to the host. It has been shown that endosymbionts influence asexual development and sporulation through the regulation of Ras2 (Mondo et al. 2017). While we observed limited changes in fungal transcription when comparing wt and cured spores, we did observe changes in the expression of fungal genes upon exposure to macrophages. In our companion paper, Itabangi et al show that the presence of an endosymbiont is important for virulence of *R. microsporus.* The endosymbiont enhances virulence through the secretion of an anti-phagocytic factor. The endosymbiont also impacts organisation of the fungal plasma membrane, as well as environmental stress resistance and resistance to macrophage-mediated killing (Itabangi et al., 2019). We show here that this is mirrored by the transcriptional response of the WT and cured spores of both *Rhizopus* species to macrophages, and in the macrophage response to infection.

As anticipated, activation of pro-inflammatory pathways increased macrophage survival in response to the spores. This consolidates several studies which demonstrate improved innate immune cell response to fungal pathogens when primed (Rogers et al. 2013; Municio et al. 2013; Blasi et al. 1995). It has been shown that the early immune response to a *Mucor circinelloides* infection is dependent on the formation of a pro-inflammatory TNF-α-expressing granuloma-like structure that controls but does not kill spores in the zebrafish model (Inglesfield et al. 2018). Ungerminated *Rhizopus* spores are highly resistant to ROS/RNS which may mediate survival within granulomata. Consistent with this, the induction of a strong proinflammatory response by cured *R. microsporus*, hypersensitive to ROS/RNS stress, allows macrophages to better control the spores.

Interestingly, we see the chitin synthase inhibitor, Nikkomycin Z, is able to inhibit germination in both *R. delemar* and *R. microsporus*. This demonstrates the requirement of chitin synthase for spore development in these species. Treated spores swell, but do not polarise. The ability to germinate also has consequences for virulence. The ability of macrophages to control swollen spores, but not subsequently polarised ones, highlights that the developmental stage of the spore is key to innate immune success and control. Whilst many fungal pathogens are virulent in an ungerminated form, germination appears a key virulence factor for these filamentous fungi. This is confirmed by work which shows that the developmental stage of both *R. microsporus* and *Rhizopus oryzae* spores impacts pathogenesis in zebrafish and murine models (Itabangi et al., 2019; Andrianaki et al., 2018).

417 Specifically, infection with pre-swollen spores leads to evasion of macrophage-mediated
418 immunity and increased pathogenesis (Itabangi et al., 2019; Andrianaki et al., 2018). In both
419 models, spore clearance is dependent on phagocyte recruitment, and we show that
420 phagocyte recruitment (in Itabangi et al.) and activation (Figure 7) is influenced by
421 endosymbiont status (Itabangi et al., 2019; Andrianaki et al., 2018). In addition, we
422 extended this analysis by revealing profound differences in the host response to two closely
423 related *Rhizopus* species. In particular, we observe a M2/damage-associated response
424 during infection with wt *R. delemar* spores that is shifted towards an M1 protective
425 response upon infection with cured *R. microsporus* spores. We reinforce this finding through
426 experimental modulation of macrophage polarization, showing that exposure to strongly
427 M1-polarizing LPS is sufficient to reduce macrophage killing by wt *R. delemar* spores.
428 Therefore, our data provide a framework for beginning to understand differences in the
429 relative virulence of pathogenic Mucorales species and underpin our finding of cross-
430 kingdom fungal-bacterial symbiosis influencing mammalian disease.
431

432 Methods

433

434 Fungal Culture

435 *R. delemar* and *R. microsporus* were cultured with Sabouraud dextrose agar (SDA) or broth
436 (10 g/liter mycological peptone, 20 g/liter dextrose), sourced from Sigma-Aldrich, at room
437 temperature. Spores were harvested, 10 days after plating, with phosphate-buffered saline
438 (PBS), centrifuged for 3 min at 3,000 rpm, and washed. Appropriate concentrations of
439 spores were used for further experiments as indicated. To cure spores of their respective
440 bacterial endosymbionts, spores were cultured with ciprofloxacin, as described in Itabangi
441 et al. 2019. Once cured, spores were subcultured at least twice in ciprofloxacin-free media
442 before use.

443 Macrophage Culture

444 Macrophages from the J774.A1 cell line were cultured in Dulbecco's Modified Eagle
445 Medium, (complemented with 10% foetal bovine serum, 1% penicillin, 1% streptomycin and
446 1% L-glutamine). Macrophages were grown at 37°C, in 5% CO_2.
447

448 Phagocytosis Assay

449 Macrophages were incubated for one hour in serum-free DMEM prior to infection. Spores
450 were pre-swollen in SAB (2 hr for *R. delemar,* 4 hr for *R. microsporus).* Washed spores were
451 incubated at 5:1 MOI with 1 x 10^5 macrophages as described in Itabangi et al, to ensure that
452 >95% of macrophages contained one spore or more. After a 1 hour of incubation, excess
453 spores were washed off the surface and the macrophages were incubated for a further 2
454 hours, before processing for RNA-Seq experiments. For live cell imaging experiments,
455 images were taken starting immediately after the excess spores were removed.
456

457 Live Cell Imaging

458 Time course images were taken to determine how LPS pre-treatment (100ng/ml) (Myers et
459 al. 2010) of macrophages, and Nikkomycin Z pre-treatment (120ug/ml over the course of
460 swelling in SAB) of spores effected phagocytic outcome. Images were taken at 20x on a Zeiss
461 Axio Observer, with images taken every 5 minutes. Bright-field and fluorescent images were

462 then analysed using ImageJ V1.

463 Comparative Genomics and Enrichment Analysis

464 Fishers exact test was used to detect enrichment of Pfam terms between *R. delemar* and *R.*
465 *microsporus*, terms with a corrected P value of < 0.01 were considered significant.
466 Orthologue genes of *R. delemar* and *R. microsporus* were identified using blast+. R (version
467 3.3.3) was used to carry out hypergeometric testing of KEGG and GO terms to determine
468 enrichment.
469

470 Bulk RNA-Seq

471 RNA was extracted from spores which had either been incubated with the macrophages, or
472 incubated in DMEM for the equivalent time period. To remove the macrophages, triton at
473 1% was used to lyse the macrophages, the resulting solution was then centrifuged for 3 min
474 at 3,000 rpm, and washed, leaving only spores. The DMEM control also received the same
475 treatment. To extract total RNA, the washed samples were immediately immersed in TRIzol
476 and lysed via bead beating at 6,500rpm for 60s. Samples were then either immediately
477 frozen at -20°C and stored for RNA extraction or placed on ice for RNA extraction. After lysis,
478 0.2 ml of chloroform was added for every 1 ml of TRIzol used in the sample preparation.
479 Samples were incubated for 3 min and then spun at 12,000 *g* at 4°C for 15 min. To the
480 aqueous phase, an equal volume of 100% ethanol (EtOH) was added, before the samples
481 were loaded onto RNeasy RNA extraction columns (Qiagen). The manufacturer's
482 instructions were followed from this point onwards. RNA quality was checked by Agilent,
483 with all RNA integrity number (RIN) scores above 7 (Schroeder et al. 2006). One microgram
484 of total RNA was used for cDNA library preparation. Library preparation was done in
485 accordance with the NEBNext pipeline, with library quality checked by Agilent. Samples
486 were sequenced using the Illumina HiSeq platform; 100-bp paired-end sequencing was
487 employed (2 x 100 bp) (>10 million reads per sample).

488 Single Cell RNA-Seq

489 For single cell sequencing experiments, macrophages were infected with fungal spores, as
490 outlined above. Uninfected macrophages, used as a negative control, were treated in the
491 same manner and underwent mock washes and media changes at identical time points to
492 infected macrophages. Macrophages were isolated and released from the bottom of their
493 wells with accutase, as per manufacturer's instructions (Technologies n.d.). Once in solution,
494 the macrophages were loaded onto the 10X genomics single cell RNA sequencing pipeline
495 for single cell isolation and library preparation. In total, 1082 single cells were sequenced.
496 The libraries were sequenced on the Illumina Sequencing Platform.
497

498 Data Analysis

499 For the bulk RNA-Seq data, FastQC (version 0.11.5) was employed to ensure the quality of
500 all samples. Hisat2 (version 2.0.5) was used to align reads to the indexed genome of
501 *Rhizopus delemar* RA 88-880 (PRJNA13066, Ma et al. 2009) and the indexed genome of
502 *Rhizopus microsporus* (Mondo et al. 2017). HTSeq (version 0.8.0) was used to quantify the
503 output (Anders et al. 2015). Trinity and edgeR (Robinson et al. 2009)(version 3.16.5) were
504 then used to analyse differential expression (Grabherr et al. 2013). For the single cell RNA-
505 Seq data, the 10X genomics analysis pipeline (Loupe Cell Browser V 2.0.0, Cell Ranger
506 Version V 2.0.0) was used to align reads to the *mus musculus* genome (version MM10), and

quantify the output. For single cell analysis, the samples were then aggregated using this pipeline, to allow comparisons between samples.

Data Availability

Data will be available upon request.

Acknowledgments

We are grateful to the University of Birmingham's Genomics Services Facility and to Deborah Croom-Carter for her technical support.

Author contributions

PSC conceived and designed the experiments, collected the data, performed the analysis and interpretation, and wrote the manuscript. JFM, KV and CAC contributed to interpretation of the data, and contributed to the manuscript. ERB conceived and designed the experiments, contributed to interpretation of the data, and wrote the manuscript.

Funding

PSC was supported by a BBSRC MIBTP PhD Studentship (BB/M01116X/1). This work was supported by a Wellcome Trust Seed award to KV (108387/Z/15/Z). HI was supported by the Wellcome Trust Strategic Award in Medical Mycology and Fungal Immunology (097377). CAC and JFM were funded by the National Institute of Allergy and Infectious Diseases, National Institutes of Health, under award U19AI110818 to the Broad Institute. ERB was supported by the UK Biotechnology and Biological Research Council (BB/M014525/1) and a Sir Henry Dale Fellowship jointly funded by the Wellcome Trust and the Royal Society (211241/Z/18/Z).

References

Alan, E.C. et al., 2019. An Emergent Entity: Indolent Mucormycosis of the Paranasal Sinuses . A Multicenter Study. , (2193), pp.92–100.

Anders, S., Pyl, P.T. & Huber, W., 2015. HTSeq-A Python framework to work with high-throughput sequencing data. *Bioinformatics*, 31(2), pp.166–169.

Andrianaki, A.M. et al., 2018. Iron restriction inside macrophages regulates pulmonary host defense against Rhizopus species. *Nature Communications*, 9(1). Available at: http://dx.doi.org/10.1038/s41467-018-05820-2.

Baldin, C. & Ibrahim, A.S., 2017. Molecular mechanisms of mucormycosis—The bitter and the sweet. *PLOS Pathogens*, 13(8), p.e1006408. Available at: http://dx.plos.org/10.1371/journal.ppat.1006408.

Berger, U. V. & Hediger, M.A., 2006. Distribution of the glutamate transporters GLT-1 (SLC1A2) and GLAST (SLC1A3) in peripheral organs. *Anatomy and Embryology*, 211(6), pp.595–606.

548 Blasi, E. et al., 1995. Role of nitric oxide and melanogenesis in the accomplishment of
549 anticryptococcal activity by the BV-2 microglial cell line. *Journal of Neuroimmunology*,
550 58(1), pp.111–116.

551 Chamilos, G. et al., 2008. Zygomycetes Hyphae Trigger an Early , Robust Proinflammatory
552 Response in Human Polymorphonuclear Neutrophils through Toll-Like Receptor 2
553 Induction but Display Relative Resistance to Oxidative Damage . , 52(2), pp.722–724.

554 Chibucos, M.C. et al., 2016. An integrated genomic and transcriptomic survey of
555 mucormycosis-causing fungi. *Nature Publishing Group*, 7, pp.1–11. Available at:
556 http://dx.doi.org/10.1038/ncomms12218.

557 Gerrick, K.Y. et al., 2018. Transcriptional profiling identifies novel regulators of macrophage
558 polarization. *Plos One*, 13(12), p.e0208602. Available at:
559 http://dx.plos.org/10.1371/journal.pone.0208602.

560 Ghuman, H. & Voelz, K., 2017. Innate and Adaptive Immunity to Mucorales. *Journal of Fungi*,
561 3(4), p.48. Available at: http://www.mdpi.com/2309-608X/3/3/48.

562 Grabherr, M.G.., Brian J. Haas, Moran Yassour Joshua Z. Levin, Dawn A. Thompson, Ido Amit,
563 Xian Adiconis, Lin Fan, Raktima Raychowdhury, Qiandong Zeng, Zehua Chen, Evan
564 Mauceli, Nir Hacohen, Andreas Gnirke, Nicholas Rhind, Federica di Palma, Bruce W., N.
565 & Friedman, and A.R., 2013. Trinity: reconstructing a full-length transcriptome without
566 a genome from RNA-Seq data. *Nature Biotechnology*, 29(7), pp.644–652.

567 Hoffmann, K. et al., 2013. The family structure of the Mucorales: a synoptic revision based
568 on comprehensive multigene-genealogies. , pp.57–76.

569 Hou, Y. et al., 2014. The inhibitory effect of IFN-gamma on protease HTRA1 expression in
570 rheumatoid arthritis. *Journal of immunology (Baltimore, Md.: 1950)*, 193(1), pp.130–
571 138.

572 Ibrahim, A.S. et al., 2008. Bacterial endosymbiosis is widely present among zygomycetes but
573 does not contribute to the pathogenesis of mucormycosis. *The Journal of infectious*
574 *diseases*, 198(7), pp.1083–1090.

575 Inglesfield et al., 2018. Robust Phagocyte Recruitment Controls the Opportunistic Fungal
576 Pathogen Mucor circinelloides in Innate Granulomas In Vivo. , 9(2), pp.1–20.

577 Kobayashi, D.Y. & Crouch, J.A., 2009. Bacterial/Fungal interactions: from pathogens to
578 mutualistic endosymbionts. *Annual review of phytopathology*, 47, pp.63–82.

579 Kraibooj, K. et al., 2014. Virulent strain of Lichtheimia corymbifera shows increased
580 phagocytosis by macrophages as revealed by automated microscopy image analysis.
581 *Mycoses*, 57(s3), pp.56–66.

582 Liu, M. et al., 2018. Comparative genome-wide analysis of extracellular small RNAs from the
583 mucormycosis pathogen Rhizopus delemar. *Scientific Reports*, 8(1), p.5243. Available
584 at: http://www.nature.com/articles/s41598-018-23611-z.

585 Luckett-Chastain, L. et al., 2016. IL-6 influences the balance between M1 and M2
586 macrophages in a mouse model of irritant contact dermatitis. *The Journal of*
587 *Immunology*, 196(1 Supplement), p.196.17--196.17. Available at:
588 http://www.jimmunol.org/content/196/1_Supplement/196.17.

589 Ma, L.J. et al., 2009. Genomic analysis of the basal lineage fungus Rhizopus oryzae reveals a
590 whole-genome duplication. *PLoS Genetics*, 5(7).

591 Martinez, F.O. et al., 2013. Genetic programs expressed in resting and IL-4 alternatively
592 activated mouse and human macrophages: similarities and differences. *Blood*, 121(9),
593 pp.e57-69.

594 Mendoza, L. et al., 2014. Human Fungal Pathogens of Mucorales and Entomophthorales.
595 *Cold Spring Harbor perspectives in medicine*, 10(1101). Available at:
596 http://perspectivesinmedicine.cshlp.org/.

597 Mondo, S.J. et al., 2017. Bacterial endosymbionts influence host sexuality and reveal
598 reproductive genes of early divergent fungi. *Nature Communications*, 8(1), p.1843.
599 Available at: https://doi.org/10.1038/s41467-017-02052-8.

600 Municio, C. et al., 2013. The Response of Human Macrophages to β-Glucans Depends on the
601 Inflammatory Milieu. *PLoS ONE*, 8(4).

602 Muñoz, J.F. et al., 2018. Coordinated host-pathogen transcriptional dynamics revealed using
603 sorted subpopulations and single, Candida albicans infected macrophages. *bioRxiv*,
604 p.350322. Available at: http://biorxiv.org/content/early/2018/06/19/350322.abstract.

605 Myers, J.T., Tsang, A.W. & Swanson, J.A., 2010. Activation of Murine Macrophages. *Current*
606 *Protocols Immunology*, 171(10), pp.5447–5453.

607 Owen, J.L. & Mohamadzadeh, M., 2013. Macrophages and chemokines as mediators of
608 angiogenesis. *Frontiers in Physiology*, 4 JUL(July), pp.1–8.

609 Petraitis, V. et al., 2013. Increased virulence of Cunninghamella bertholletiae in
610 experimental pulmonary mucormycosis: correlation with circulating molecular
611 biomarkers, sporangiospore germination and hyphal metabolism. *Medical mycology*,
612 51(1), pp.72–82.

613 Raggi, F. et al., 2017. Regulation of human Macrophage M1-M2 Polarization Balance by
614 hypoxia and the Triggering receptor expressed on Myeloid cells-1. *Frontiers in*
615 *Immunology*, 8(SEP), pp.1–18.

616 Robinson, M.D., McCarthy, D.J. & Smyth, G.K., 2009. edgeR: A Bioconductor package for
617 differential expression analysis of digital gene expression data. *Bioinformatics*, 26(1),
618 pp.139–140.

619 Rogers, H. et al., 2013. Role of bacterial lipopolysaccharide in enhancing host immune
620 response to candida albicans. *Clinical and Developmental Immunology*, 2013.

621 Schmidt, S. et al., 2013. Immunobiology Rhizopus oryzae hyphae are damaged by human

natural killer (NK) cells , but suppress NK cell mediated immunity. *Immunobiology*, 218(7), pp.939–944. Available at: http://dx.doi.org/10.1016/j.imbio.2012.10.013.

Schroeder, A. et al., 2006. The RIN: an RNA integrity number for assigning integrity values to RNA measurements. *BMC molecular biology*, 7(1), p.3. Available at: http://www.pubmedcentral.nih.gov/articlerender.fcgi?artid=1413964&tool=pmcentrez&rendertype=abstract.

Schwartze, V.U. et al., 2014. Gene Expansion Shapes Genome Architecture in the Human Pathogen Lichtheimia corymbifera: An Evolutionary Genomics Analysis in the Ancient Terrestrial Mucorales (Mucoromycotina). *PLoS Genetics*, 10(8).

Sephton-Clark, P.C.S. et al., 2018. Pathways of Pathogenicity: Transcriptional Stages of Germination in the Fatal Fungal Pathogen Rhizopus delemar. *mSphere*, 3(5), pp.1–16.

Spellberg, B., Edwards, J. & Ibrahim, A., 2016. Novel Perspectives on Mucormycosis: Pathophysiology , Presentation , and Management. , 18(3), pp.556–569.

Szulzewsky, F. et al., 2015. Glioma-associated microglia/macrophages display an expression profile different from M1 and M2 polarization and highly express Gpnmb and Spp1. *PLoS ONE*, 10(2), pp.1–27.

Technologies, S., Accutase Directions For Use. Available at: https://cdn.stemcell.com/media/files/pis/29637-PIS_1_0_2.pdf?_ga=2.10286005.1436903603.1548350382-38118485.1548350382.

van Tol, S. et al., 2017. The TRIMendous Role of TRIMs in Virus–Host Interactions. *Vaccines*, 5(3), p.23. Available at: http://www.mdpi.com/2076-393X/5/3/23.

Warris, A. et al., 2005. Cytokine responses and regulation of interferon-gamma release by human mononuclear cells to Aspergillus fumigatus and other filamentous fungi. , (November), pp.613–621.

Ye, R.D. & Sun, L., 2015. Emerging functions of serum amyloid A in inflammation. *Journal of Leukocyte Biology*, 98(6), pp.923–929. Available at: http://www.jleukbio.org/cgi/doi/10.1189/jlb.3VMR0315-080R.

Figure legends

Figure 1 Phenotypic and genomic comparisons. A) Experimental setup: Pre-swollen (Sab) WT or cured fungal spores from *Rhizopus delemar* (2hr) and *Rhizopus microsporus* (4hr) in mid-isotropic phase were co-cultured with J774.1 murine macrophages (sfDMEM) at 5:1 MOI for 1hr, washed to remove unengulfed spores, then co-incubated for a further 2 hr and RNA for fungi and host cells harvested. Pre-swollen spores (Sab) incubated in sfDMEM for 3hr served as the negative control. B) Germination percentage over time for *R. delemar* and *R. microsporus* grown in Sab. C) Spore sizes for *R. delemar* and *R. microsporus* grown in SAB. D) Pfam terms enriched (corrected $P < 0.01$) in *R. delemar* vs *R. microsporus* genomes, with

660 colour indicating the extent of enrichment (Log_{10} Count).

661 **Figure 2 Principal component analysis of fungal genes differentially expressed across all**
662 **samples.** A) *R. delemar* wt and cured, macrophage engulfed or sfDMEM control B) *R.*
663 *microsporus* wt and cured, macrophage engulfed or sfDMEM control. Replicates (n=3) are
664 shown for each sample.

665 **Figure 3 Clustering of fungal transcriptional changes.** A) Heatmap displaying differentially
666 expressed genes in *R. delemar*. Expression levels are plotted in Log2, space and mean-
667 centered (FDR < 0.001) B) Heatmap displaying differentially expressed genes in *R.*
668 *microsporus*. Expression levels are plotted in Log2, space and mean-centered (FDR < 0.001)

669 **Figure 4 Differential expression of fungal genes in compared conditions**. A) The number of
670 genes significantly differentially expressed (multiple corrected P value < 0.05) between
671 samples. Blue bars indicate genes with an increase in expression (LogFC > 2), whilst orange
672 bars indicate genes with a decrease in expression (LogFC < -2).

673 **Figure 5 Gene functions of genes differentially expressed in *R. delemar*.** Enriched KEGG
674 categories for the up/down regulated genes over sample comparisons. The enrichment of
675 the category is indicated by the colour bar. White corresponds to no enrichment, and yellow
676 to red corresponds to the given P value of the enrichment.

677 **Figure 6 Principal component analysis of macrophage genes differentially expressed**
678 **across all samples.** Single cell sequencing was performed on uninfected and infected
679 macrophages. Transcriptional data from the experiment was analysed with the 10X
680 genomics analysis pipeline, and aggregated prior to principle component analysis.

681 **Figure 7 Clustering of macrophage transcription.** Heatmap displaying immune response
682 genes significantly differentially expressed between macrophage populations. Expression
683 levels are plotted in Log2 (FDR < 0.001)

684 **Figure 8 Macrophage survival following exposure to *R. delemar* and *R. microsporus* spores.**
685 Macrophages +/- LPS pre-treatment were infected (MOI 5:1) with fungal spores, pre-swollen
686 in SAB consistent with single cell experiments. Macrophages were infected with fungal
687 spores that were pre-treated with +/- Nikkomycin Z (24 μg/ml; n=3 for each sample).
688 Macrophage survival was determined 7 hr post infection. Significant differences between
689 samples is indicated by (*= p < 0.01).

690 **Supplementary Figure 1** Table of Pfam terms found to be enriched (corrected $P < 5 \times 10^{-8}$) in
691 *R. delemar* and *R. microsporus* upon genome comparison.

692 **Supplementary Figure 2 Clustering of fungal transcription with GO annotation**. Heatmap
693 displaying all differentially expressed genes, across all conditions, in *R. microsporus*.
694 Expression levels are plotted in Log2, space and mean-centered (FDR < 0.001).

695 **Supplementary Figure 3 Clustering and heterogeneity in single cell analysis of J774.1**
696 **macrophages.** Single cell plot generated by loupe cell browser. Colors indicate experimental
697 conditions as indicated. Spacial distribution indicates relative similarity across all detected
698 transcripts. 1082 single cells represented.

699 **Supplementary Figure 4 Expression of chitin synthase genes**. A) Heatmap showing the
700 expression of chitin synthase genes in *R. delemar* B) Heatmap showing the expression of
701 chitin synthase genes in *R. microsporus*

702 **Supplementary Figure 5 Chitin synthase inhibition of *R. delemar* and *R. microsporus***
703 **germination**. *R. delemar* and *R. microsporus* treated with Nikkomycin Z in SAB at indicated
704 concentrations for the indicated times. Fluorescence indicates calcofluor white staining, and
705 thus the availability of chitin/chitosan in the cell wall. Labels indicate time and
706 concentration of inhibitor.

707 **Supplemental Table 1** Selected genes differentially regulated in pairwise comparisons, with
708 Pfam annotations provided where available.

709 **Supplementary Table 2** Table displaying the LogFC values for a subset of genes displayed in
710 Figure 7.

711

A

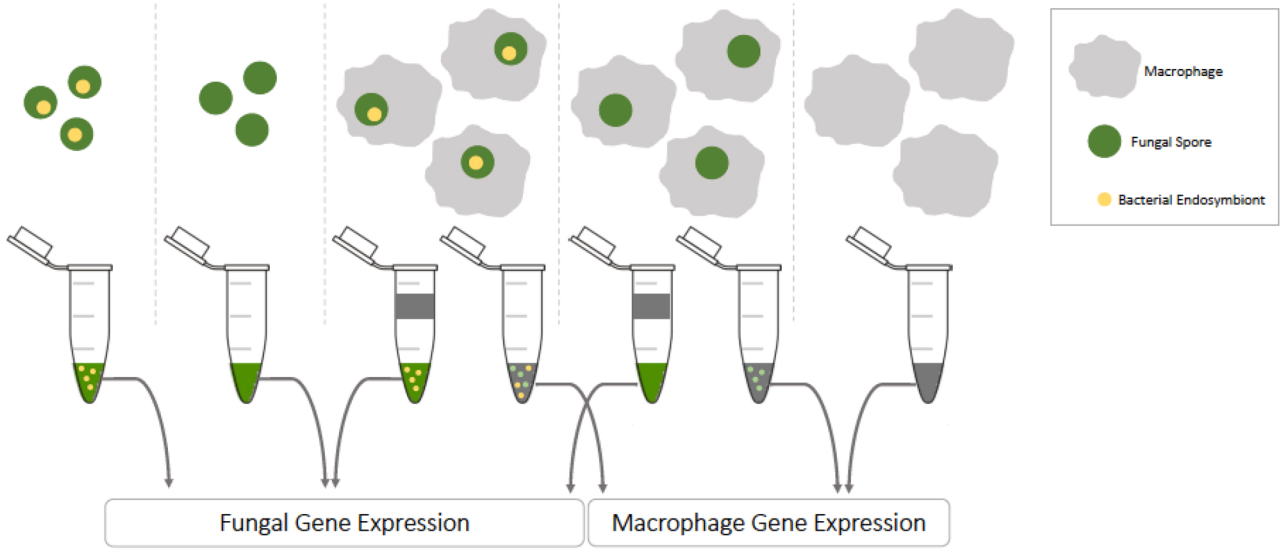
Macrophage
Fungal Spore
Bacterial Endosymbiont
Fungal Gene Expression
Macrophage Gene Expression

B

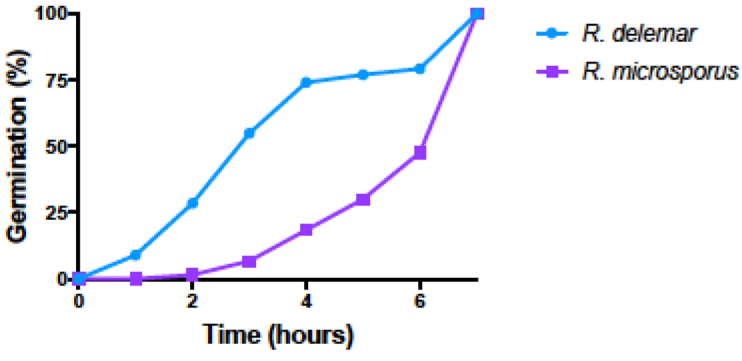
Germination (%)
100
75
50
25
0
0
2
4
6
Time (hours)
R. delemar
R. microsporus

C

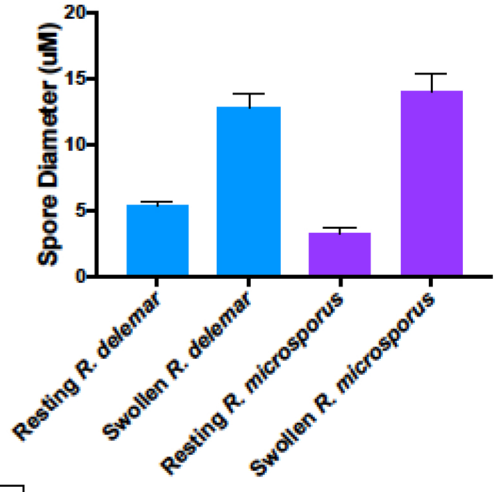
Spore Diameter (uM)
20
15
10
5
0
Resting R. delemar
Swollen R. delemar
Resting R. microsporus
Swollen R. microsporus

D

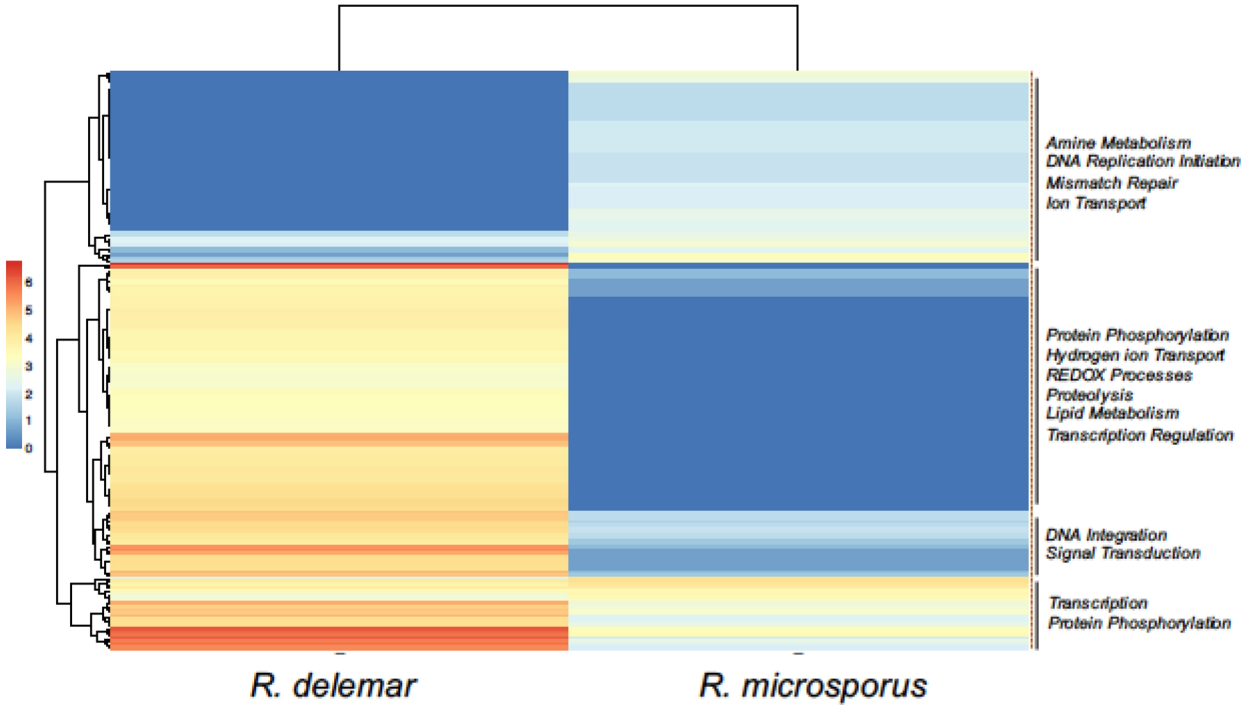
6
5
4
3
2
1
0
Amine Metabolism
DNA Replication Initiation
Mismatch Repair
Ion Transport
Protein Phosphorylation
Hydrogen ion Transport
REDOX Processes
Proteolysis
Lipid Metabolism
Transcription Regulation
DNA Integration
Signal Transduction
Transcription
Protein Phosphorylation
R. delemar
R. microsporus

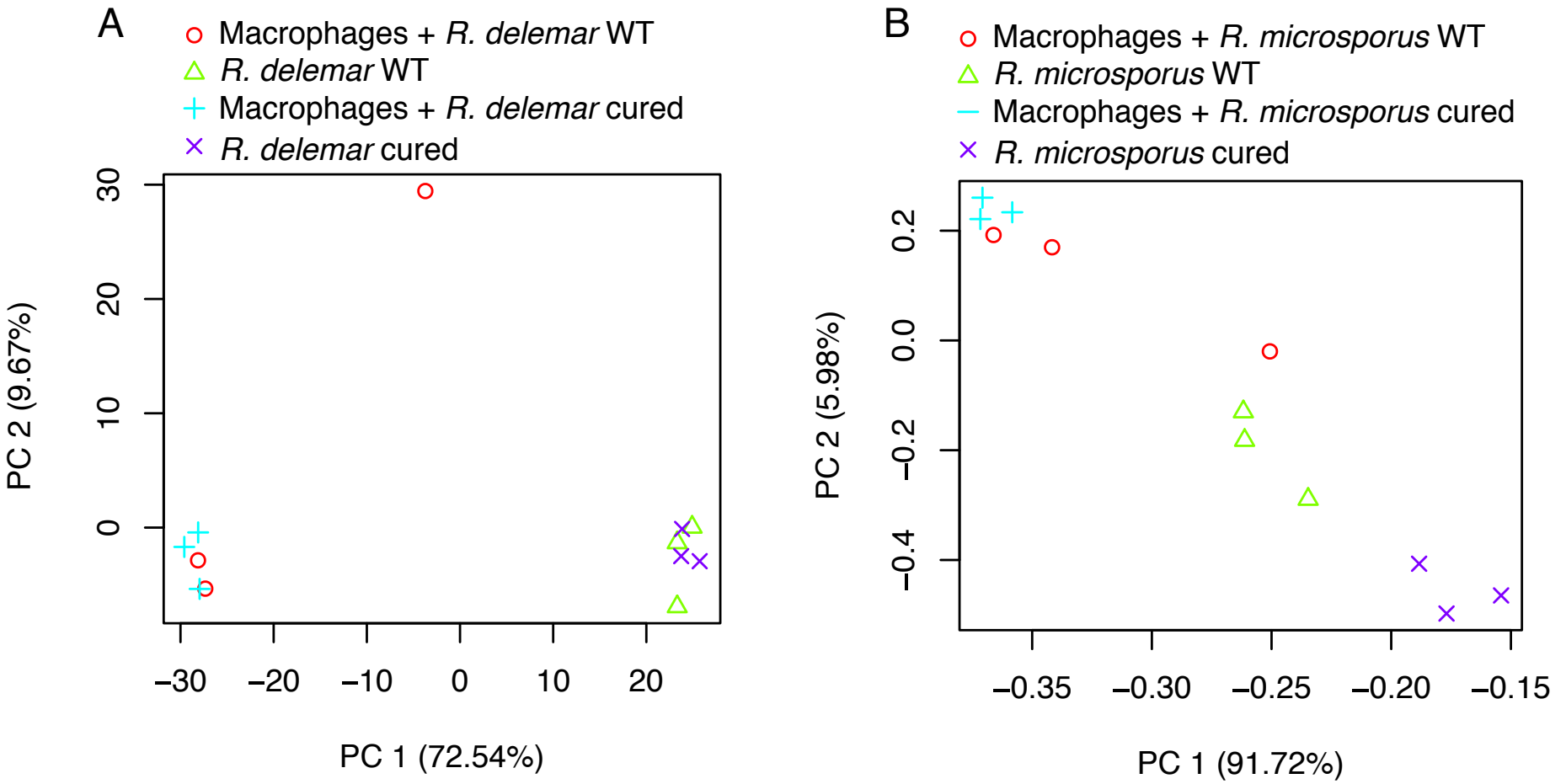
A
Macrophages + R. delemar WT
R. delemar WT
Macrophages + R. delemar cured
R. delemar cured
PC 2 (9.67%)
PC 1 (72.54%)
30
20
10
0
−30
−20
−10
0
10
20
B
Macrophages + R. microsporus WT
R. microsporus WT
Macrophages + R. microsporus cured
R. microsporus cured
PC 2 (5.98%)
PC 1 (91.72%)
0.2
0.0
−0.2
−0.4
−0.35
−0.30
−0.25
−0.20
−0.15

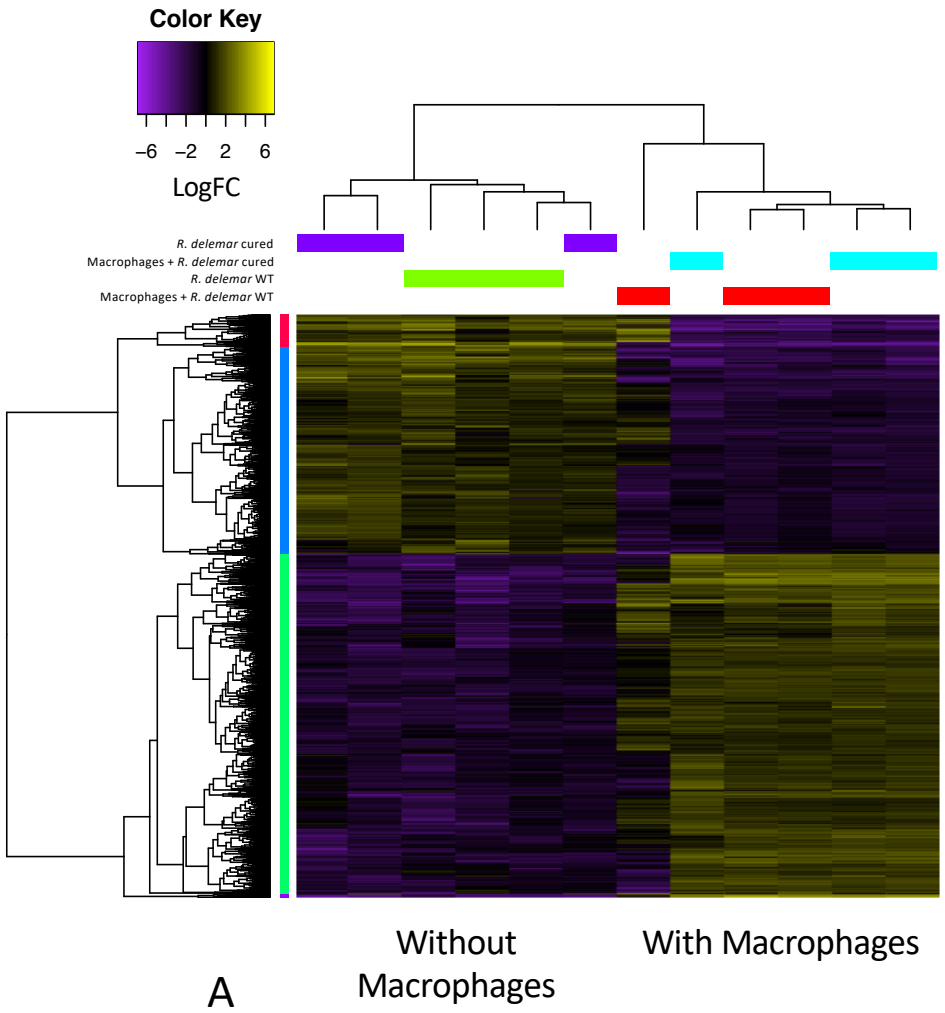
Color Key
−6 −2 2 6
LogFC
R. delemar cured
Macrophages + R. delemar cured
R. delemar WT
Macrophages + R. delemar WT
Without Macrophages
With Macrophages
A

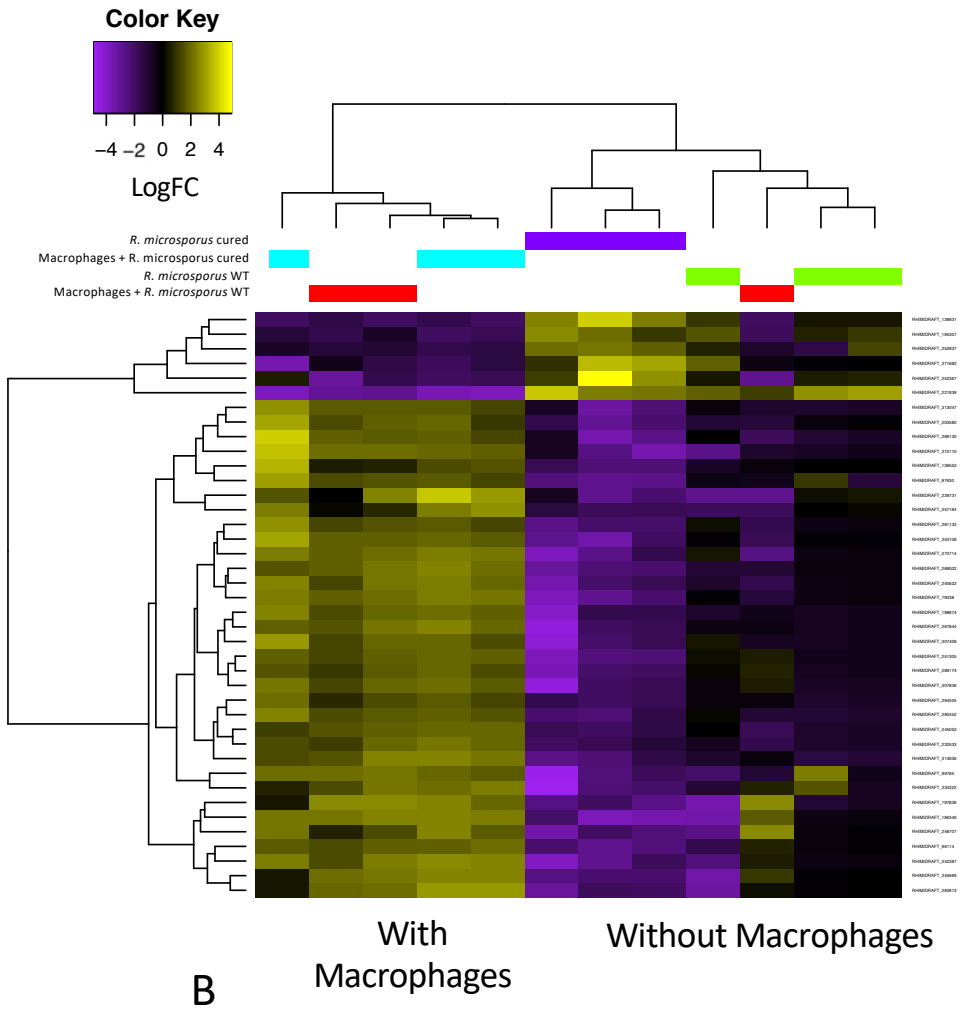
Color Key
−4 −2 0 2 4
LogFC
R. microsporus cured
Macrophages + R. microsporus cured
R. microsporus WT
Macrophages + R. microsporus WT
With Macrophages
Without Macrophages
B

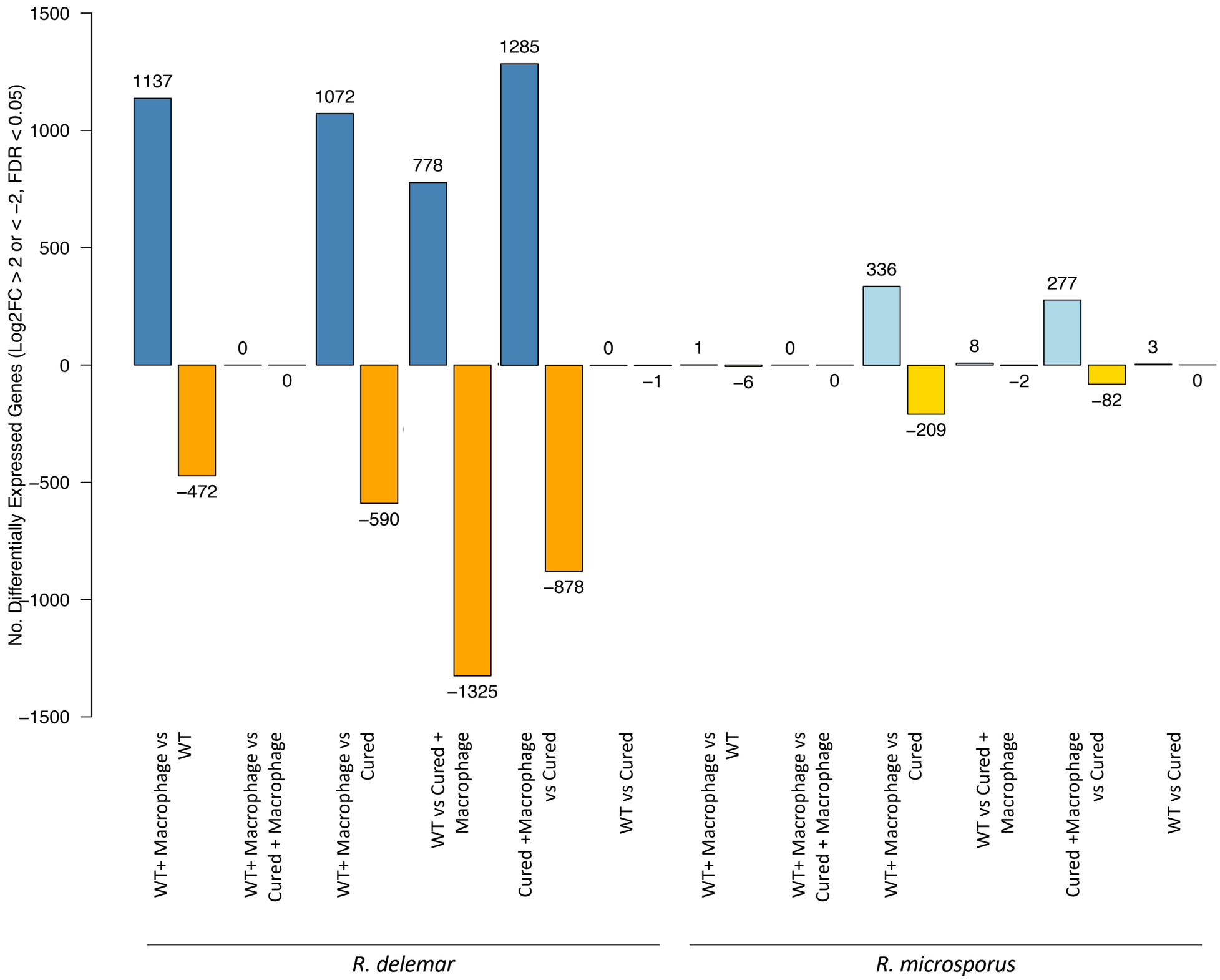
No. Differentially Expressed Genes (Log2FC > 2 or < −2, FDR < 0.05)
1500
1000
500
0
−500
−1000
−1500
1137
−472
0
0
1072
−590
778
−1325
1285
−878
0
−1
1
−6
0
0
336
−209
8
−2
277
−82
3
0
WT+ Macrophage vs WT
WT+ Macrophage vs Cured + Macrophage
WT+ Macrophage vs Cured
WT vs Cured + Macrophage
Cured +Macrophage vs Cured
WT vs Cured
WT+ Macrophage vs WT
WT+ Macrophage vs Cured + Macrophage
WT+ Macrophage vs Cured
WT vs Cured + Macrophage
Cured +Macrophage vs Cured
WT vs Cured
R. delemar
R. microsporus

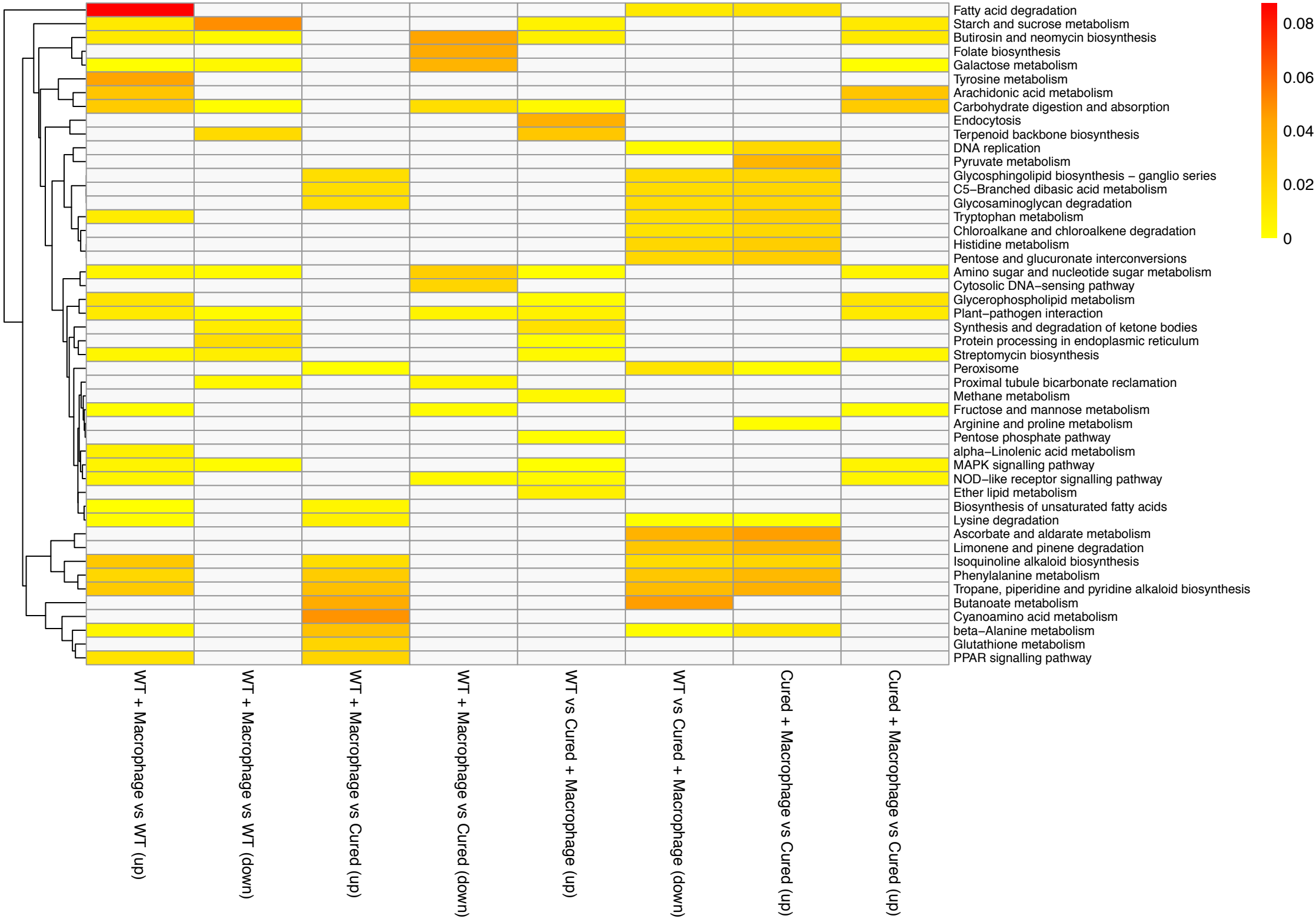
Fatty acid degradation
Starch and sucrose metabolism
Butirosin and neomycin biosynthesis
Folate biosynthesis
Galactose metabolism
Tyrosine metabolism
Arachidonic acid metabolism
Carbohydrate digestion and absorption
Endocytosis
Terpenoid backbone biosynthesis
DNA replication
Pyruvate metabolism
Glycosphingolipid biosynthesis – ganglio series
C5–Branched dibasic acid metabolism
Glycosaminoglycan degradation
Tryptophan metabolism
Chloroalkane and chloroalkene degradation
Histidine metabolism
Pentose and glucuronate interconversions
Amino sugar and nucleotide sugar metabolism
Cytosolic DNA–sensing pathway
Glycerophospholipid metabolism
Plant–pathogen interaction
Synthesis and degradation of ketone bodies
Protein processing in endoplasmic reticulum
Streptomycin biosynthesis
Peroxisome
Proximal tubule bicarbonate reclamation
Methane metabolism
Fructose and mannose metabolism
Arginine and proline metabolism
Pentose phosphate pathway
alpha–Linolenic acid metabolism
MAPK signalling pathway
NOD–like receptor signalling pathway
Ether lipid metabolism
Biosynthesis of unsaturated fatty acids
Lysine degradation
Ascorbate and aldarate metabolism
Limonene and pinene degradation
Isoquinoline alkaloid biosynthesis
Phenylalanine metabolism
Tropane, piperidine and pyridine alkaloid biosynthesis
Butanoate metabolism
Cyanoamino acid metabolism
beta–Alanine metabolism
Glutathione metabolism
PPAR signalling pathway
WT + Macrophage vs WT (up)
WT + Macrophage vs WT (down)
WT + Macrophage vs Cured (up)
WT + Macrophage vs Cured (down)
WT vs Cured + Macrophage (up)
WT vs Cured + Macrophage (down)
Cured + Macrophage vs Cured (up)
Cured + Macrophage vs Cured (up)
0.08
0.06
0.04
0.02
0

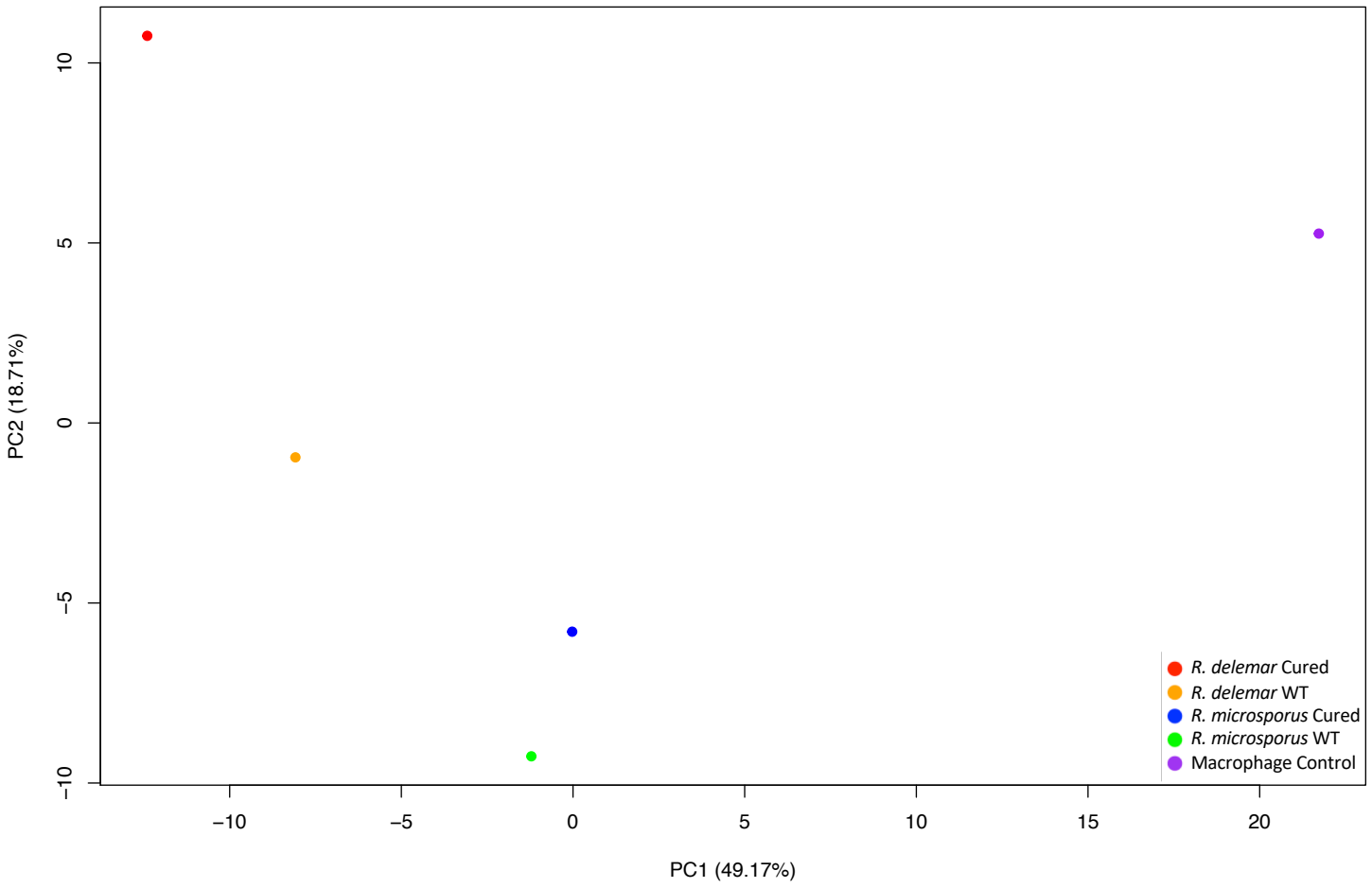
PC2 (18.71%)
PC1 (49.17%)
10
5
0
−5
−10
−10
−5
0
5
10
15
20
R. delemar Cured
R. delemar WT
R. microsporus Cured
R. microsporus WT
Macrophage Control

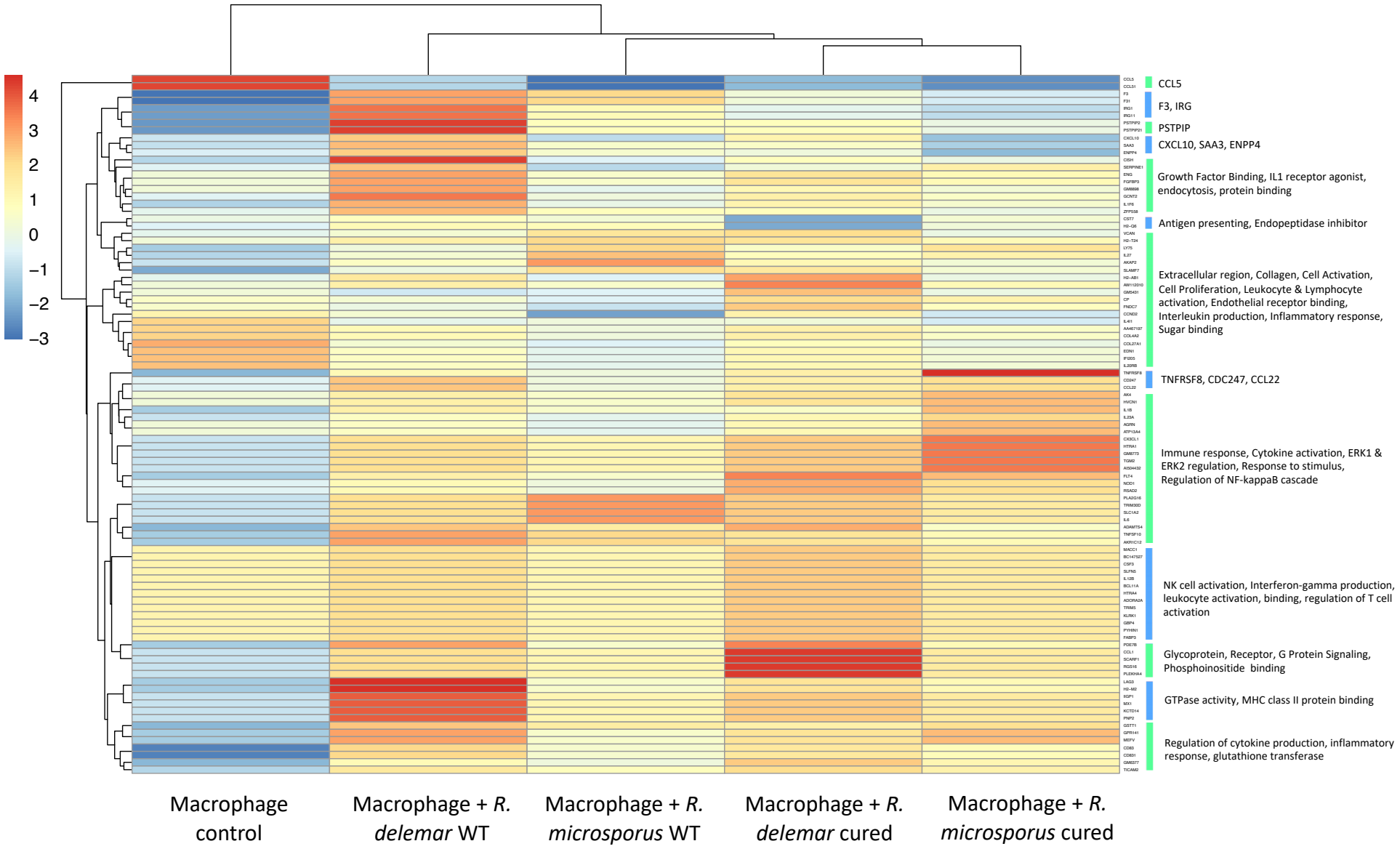
4
3
2
1
0
−1
−2
−3
CCL5
F3, IRG
PSTPIP
CXCL10, SAA3, ENPP4
Growth Factor Binding, IL1 receptor agonist, endocytosis, protein binding
Antigen presenting, Endopeptidase inhibitor
Extracellular region, Collagen, Cell Activation, Cell Proliferation, Leukocyte & Lymphocyte activation, Endothelial receptor binding, Interleukin production, Inflammatory response, Sugar binding
TNFRSF8, CDC247, CCL22
Immune response, Cytokine activation, ERK1 & ERK2 regulation, Response to stimulus, Regulation of NF-kappaB cascade
NK cell activation, Interferon-gamma production, leukocyte activation, binding, regulation of T cell activation
Glycoprotein, Receptor, G Protein Signaling, Phosphoinositide binding
GTPase activity, MHC class II protein binding
Regulation of cytokine production, inflammatory response, glutathione transferase
Macrophage control
Macrophage + *R. delemar* WT
Macrophage + *R. microsporus* WT
Macrophage + *R. delemar* cured
Macrophage + *R. microsporus* cured

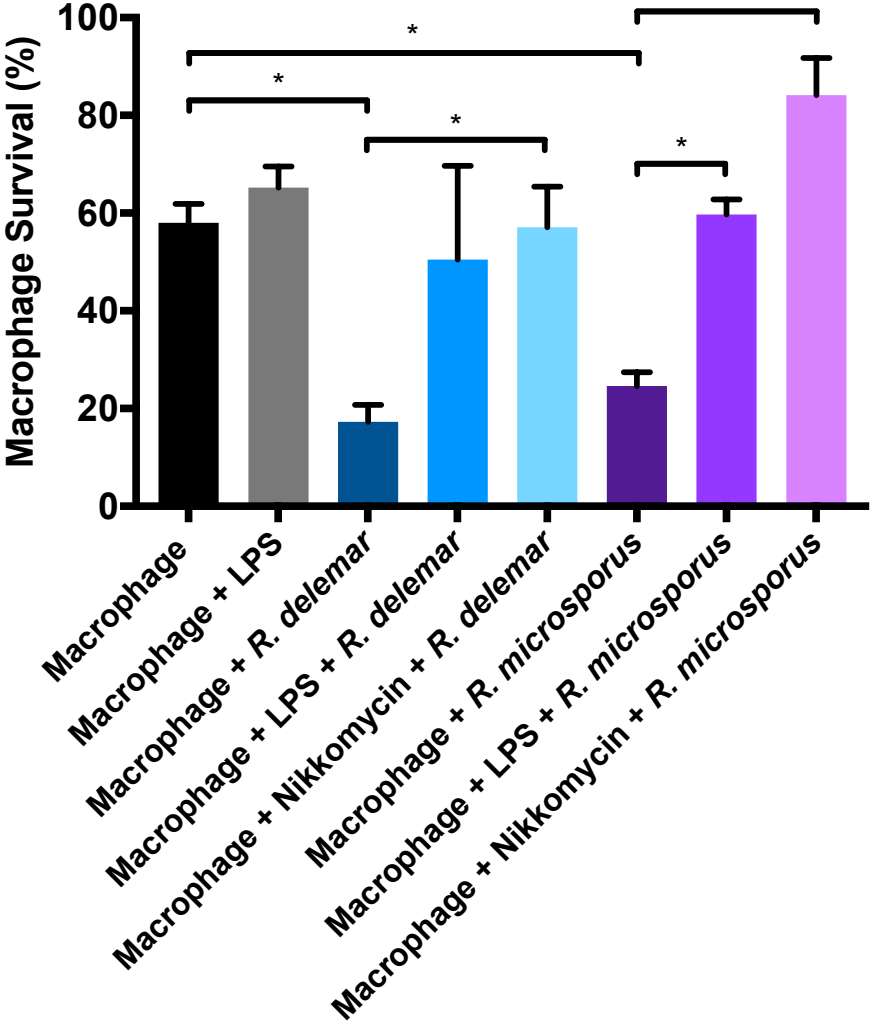
Macrophage Survival (%)
100
80
60
40
20
0
*
*
*
*
*
Macrophage
Macrophage + LPS
Macrophage + R. delemar
Macrophage + LPS + R. delemar
Macrophage + Nikkomycin + R. delemar
Macrophage + R. microsporus
Macrophage + LPS + R. microsporus
Macrophage + Nikkomycin + R. microsporus